



Cite this: DOI: 10.1039/c7dt03142d

Pushing the photodelivery of nitric oxide to the visible: are {FeNO}⁷ complexes good candidates?†

 Natalia Levin,^a Julián Perdomónico,^a Eckhard Bill,^b Thomas Weyhermüller^b
and Leonardo D. Slep^{a*}

Photodelivery of NO requires stable compounds which can be made reactive by irradiation with (visible) light. Traditional {MNO}⁶ complexes require a substantial ligand design to shift their absorption spectra to the appropriate region of the electromagnetic spectrum. [Fe((CH₂Py)₂Me[9]aneN₃(NO))(BF₄)₂] is a new {FeNO}⁷ octahedral coordination compound, which is thermally and air-stable in solution. Illumination with a 450 nm light source induces significant photodetachment of the coordinated NO ($\phi_{\text{NO}} = 0.52$ mol einstein⁻¹), suggesting that {FeNO}⁷ compounds can be in fact suitable compounds for therapeutic NO-photorelease.

 Received 24th August 2017,
Accepted 26th October 2017

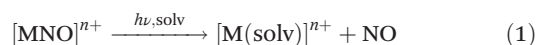
DOI: 10.1039/c7dt03142d

rsc.li/dalton

Introduction

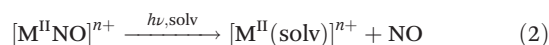
NO releasing compounds were already used therapeutically for the treatment of illnesses¹ long before the discovery of the multiple physiological activities that nitric oxide (NO) presents in mammals,² and before the proposal of an endogenous synthetic path for it.³ The findings of the role of NO in cellular apoptosis in the early 1990s promoted the search of appropriate NO-releasing molecules for use in antitumor therapies. One of the strategies developed was focused on designing NO-photoreleasing species to be employed in photodynamic therapy (PDT).⁴ The quest for robust nitrosyl metallic complexes thermally stable under physiological conditions and sensitive only to a specific incident irradiation source (if possible in the visible range of the spectrum) while having at the same time high quantum yields of NO release (ϕ_{NO}) fuelled the field of photochemistry of inorganic nitrosyl complexes.⁵ In this regard, ruthenium nitrosyls emerged as good candidates and have been the main focus of this kind of investigation, particularly constrained to {RuNO}⁶ species, due to their stability towards O₂ and ease of manipulation.^{5,6} The abundant literature on the subject offers a general consensus through which the release of a NO molecule involves the popu-

lation of a ³MLCT state that leads to the generation of an unstable intermediate {Ru^{III}-NO[•]} and finally of the photoproduct [Ru^{III}-solv]ⁿ⁺ (eqn (1)).



The strong π -acceptor nature of the nitrosyl moiety in {MNO}⁶ species is responsible for the main complication in this kind of substance. The covalent interaction with the t_{2g} set of metal orbitals shifts the whole absorption spectrum to the UV region making most of the known substances unsuitable for any practical application. Some of the most interesting reports on the field explore in fact creative synthetic variations intended to red-shift the absorption profile.⁷

The exploration of {MNO}ⁿ NO-releasing species with *n* greater than 6 has only scarcely appeared more recently in the literature. This is surprising, given the fact that these reduced NO holding species are expected to display lower energy electronic transitions without the need for extensive coligand design due to the lower covalency of the M–NO bond. In 2005, Sawaia *et al.* reported the photochemistry of a {RuNO}⁷ species (*cis*-[Ru(bpy)₂(4-pic)(NO)]²⁺, 4-pic = 4-picoline) generated *in situ* by electrochemical reduction in aqueous medium.⁸ We reported later the first XRD characterization of a {RuNO}⁷ complex ([Ru(Me₃[9]aneN₃)(bpy)(NO)]²⁺) whose solutions proved sensitive to a 365 nm irradiation source leading to NO release.⁹ In both cases, the processes were interpreted according to eqn (2), where the oxidation state of the metal center remains unchanged upon NO release.



To our knowledge there has been only one investigation of another {FeNO}⁷ species, [Fe(N₃PyS)(NO)]²⁺ (N₃PyS = *N,N*-bis(2-

^aDepartamento de Química Inorgánica, Analítica y Química Física, Facultad de Ciencias Exactas y Naturales, and INQUIMAE, Universidad de Buenos Aires – CONICET, Pabellón 2, 3er piso, Ciudad Universitaria, C1428EHA, Ciudad Autónoma de Buenos Aires, Argentina. E-mail: slep@qi.fcen.uba.ar

^bMax-Planck-Institut für Chemische Energiekonversion, Stiftstraße 34-36, D-45470 Mülheim an der Ruhr, Germany

† Electronic supplementary information (ESI) available. CCDC 1565106. For ESI and crystallographic data in CIF or other electronic format see DOI: 10.1039/c7dt03142d

pyridylmethyl)-(N-(bis-2-pyridylmethyl)amine)), that also shows the release of NO in acetonitrile when interacting with an irradiation source, following the same reaction stoichiometry depicted in eqn (2).¹⁰ Noticeably, the photodetachment of NO from the latter seems to be induced under low-intensity visible light, though no overall quantum yield has been reported. The lack of additional reports on {FeNO}⁷ photoactive species, combined with the fact that the compound [Fe(N₄Py)(NO)]²⁺ (N₄py = N,N-bis(2-pyridylmethyl)-N-bis(2-pyridyl)methylamine) also explored in the same report behaves as a non-photoactive species, might be wrongly considered as enough evidence to claim that [Fe(N₃PyS)(NO)]²⁺ shows an exceptional behavior, when in fact this subject has not been sufficiently explored. We report herein the synthesis and complete characterization of a new {FeNO}⁷ species holding a coordination sphere inspired from our previous report of a {RuNO}⁷ complex. The new compound, as well as its Ru analog, shows NO release photoreactivity when exposed to a 365 nm light source but also efficient photorelease of NO upon irradiation in the visible range.

Materials and experimental procedures

Materials and reagents. The reagents employed in the synthetic procedures were purchased from Sigma-Aldrich, and were used without further purification. All organic solvents employed in synthetic procedures or physical determinations were dried and freshly distilled before use following the standard procedures.¹¹ A vacuum line and Schlenk glassware (or alternatively a glovebox) were employed when the manipulation required the exclusion of air. The precursor 1,4,7-triazatricyclo[5.2.1.0^{4,10}]decane (the orthoamide of 1,4,7-triazacyclononane) of the pentadentate ligand employed in the synthesis of the complex was prepared according to an already published procedure.¹²

Synthesis of Me[9]aneN₃

The procedure was inspired by a previous report.¹³ Modifications described here simplify the synthesis without the loss of yield: 0.720 g of 1,4,7-triazatricyclo[5.2.1.0^{4,10}]decane (5.18 mmol) were dissolved in 10 mL of THF to afford a pale yellow solution. Subsequently, 1.30 g of CH₃I (9.16 mmol) were added dropwise to the mixture, upon which a white precipitate was formed that turned pale yellow over time. The reaction medium was stirred for 4 hours and the precipitate was then separated by filtration and suspended in 10 mL of water. The mixture was brought to reflux inducing the full dissolution of the solid. Once at room temperature, the yellow solution was kept at 4 °C overnight. The following day, 1.47 g of NaOH was added under stirring to the cold solution, after which the reaction mixture was refluxed for three hours. After reaching room temperature, the solution was extracted with CHCl₃ (6 × 30 mL). The combined organic layers were dried over anhydrous Na₂SO₄, filtered and evaporated in a rotavap to yield 0.526 g of a pale yellow oil (3.67 mmol, 70.9%). ¹H-NMR (Fig. S1†) (CDCl₃, 500 MHz, 298 K): δ (ppm) 2.35 (s, 3H, CH₃), 2.48 (m, 4H, CH₂), 2.68 (m, 8H, CH₂).

¹³C-DEPT-NMR (Fig. S2†) (CDCl₃, 500 MHz, 298 K): δ (ppm) 45.11 (CH₃), 54.42 (CH₂), 46.35, 45.99 (CH₂).

Synthesis of (CH₂Py₂)₂Me[9]aneN₃

The preparation of the ligand starting from Me[9]aneN₃ has been previously described.¹⁴ 0.526 g of Me[9]aneN₃ (3.67 mmol) were dissolved in 30 mL of water together with 1.22 g of picolyl chloride (7.44 mmol). The pH of the solution was brought to ca. 11 by the addition of aliquots of a 2 M solution of NaOH. The solution was stirred for three days during which the pH was kept at the same value by further additions of the basic solution. After this period, NaOH (2 M) solution was added to the mixture to achieve pH 13. Upon this, the reaction medium was extracted with CHCl₃ (6 × 30 mL). The combined organic layers were dried over anhydrous Na₂SO₄, filtered and evaporated in a rotavap to afford 0.957 g of an orange oil (2.94 mmol, 80%), which contained 90.2% of the desired compound according to a quantitative GC determination employing a RTx-5 Amine S-77 column, length 15 m and diameter 0.25 mm, along with a FID detector (Fig. S3†). The product eluted with a retention time of 23.07 min using H₂ as the gas carrier (0.42 bar, 1.7 mL min⁻¹) and a temperature ramp of 8 °C per minute starting at 70 °C until 300 °C. ¹³C-DEPT-NMR (Fig. S3†) (CD₃CN, 500 MHz, 298 K): δ = 47.13, 56.91, 58.33, 59.18, 65.78, 123.17, 124.49, 137.57, 150.02 ppm, in accordance with the ¹³C-NMR spectrum collected previously.¹⁴

Synthesis of [Fe((CH₂Py₂)₂Me[9]aneN₃)(NO)](BF₄)₂ ([1-NO](BF₄)₂)

0.99 g of Fe(BF₄)₂·5H₂O (3.10 mmol) were dissolved in a mixture of dry and degassed solvents (6 mL of methanol (MeOH) and 2 mL of acetonitrile (CH₃CN)). The initially almost colorless solution turned dark brown upon the addition of 1.12 g of (CH₂Py₂)₂Me[9]aneN₃ (3.44 mmol) pre-dissolved in 2 mL of MeOH and 1 mL of CH₃CN. After two hours of stirring, the solution was cooled down with an ice bath. NO(g) (purchased from Air Liquide, 99.5% pure, passed through a KOH(s) trap before use) was bubbled into the vigorously stirred solution, which turned immediately into a darker shade, almost black. The NO bubbling was maintained for five minutes after which Ar was circulated through the system for another ten minutes, to eliminate the excess of reagent. The ice bath was removed and the reaction medium was concentrated overnight by means of a subtle Ar flow. After this period red crystals shaped like prisms were found in the round flask surrounded by a red oil and recovered under an Ar atmosphere for XRD investigation. The oil was treated in the glove box with cold degassed solvents (3 mL MeOH and 1 mL CH₃CN) and left overnight at -30 °C under N₂ upon which a red precipitate was found in the reaction medium yielding 72.2 mg of a red solid (0.124 mmol, 39.7%). Anal. calcd for [1-NO](BF₄)₂, C₁₉H₂₇N₆O₁B₂F₈Fe (M_r = 584.92 g mol⁻¹): C 38.9, H 5.0, N 14.3. Found: C 37.8, H 4.9, N 13.7. MS (ESI⁺) (Fig. S4†) m/z: 205 = [M - 2BF₄⁻]²⁺; 190.6 = [M - NO - 2BF₄⁻]²⁺.

Physical determinations. Microanalytical data for C, H and N were obtained with a Carlo Erba EA 1108 analyzer. UV-vis spectra were recorded with either an HP8453 or an HP8452A diode array spectrophotometer. IR spectral measurements (KBr pellets) were carried out using a Nicolet iS10. The ^1H and ^{13}C NMR spectra were recorded with a 500 MHz Bruker AVANCE III spectrometer. ESI spectra were obtained with a standard ESI source and Q Exactive Plus from ThermoFisher Scientific equipment. X-band EPR spectra were recorded at 85 K with a Bruker ESP 300 spectrometer equipped with an Oxford ESR 910 liquid-helium cryostat and an Oxford temperature controller. X-band EPR spectra were simulated with EasySpin 5.0.9.¹⁸ Cyclic voltammograms were recorded in dried and degassed CH_3CN with 0.2 M of Bu_4NPF_6 as a support electrolyte in a three-electrode cell. The working electrode was a 3 mm diameter vitreous carbon disc, the counter electrode was a Pt wire and the reference electrode an Ag wire. The measured potentials were corrected by the use of an internal standard (ferrocene or decamethylferrocene).¹⁵ The potential of the working electrode was controlled with a BioLogic SP300 potentiostat. Combined controlled potential coulometry and UV-Vis spectroelectrochemistry experiments were performed in dried and degassed CH_3CN (0.1 M Bu_4NPF_6 as a support electrolyte) in a three-electrode homemade cell coupled to a quartz cuvette (1 cm path). The working electrode was a 1 cm² Pt mesh, the counter electrode was a Pt wire immersed in $\text{CH}_3\text{CN}/0.1$ M Bu_4NPF_6 and the reference electrode a Ag wire immersed in $\text{CH}_3\text{CN}/0.1$ M $\text{Bu}_4\text{NPF}_6/0.01$ M AgNO_3 . An internal ferrocene (Fc) standard was employed as a reference¹⁵ at the end of the experiments (using a 2 mm diameter vitreous carbon disc as the working electrode). The system was maintained at -20 ± 1 °C by means of an RC6 LAUDA thermostat. The potential of the working electrode was controlled with a TEQ-03 potentiostat. Photochemical experiments were performed with either 3.0 mL or 3.3 mL of solutions contained in a 1.00 cm path length fluorescence cuvette employing respectively a 365 nm or a 450 nm light emitting diode. The intensity of the 450 nm LED (2.70×10^{-6} einstein s⁻¹ dm⁻³) was determined by reference to a 365 nm LED source employing a FieldMaster-Coherent power meter with a LM-2UV photodiode as a light sensor. The 365 nm LED was calibrated by actinometry employing a standard solution of $\text{K}_3[\text{Fe}(\text{C}_2\text{O}_4)_3]$ by means of an already described procedure,¹⁶ yielding an intensity of 1.59×10^{-6} einstein s⁻¹ dm⁻³. The spectral evolution was monitored spectrophotometrically along the course of the reaction in a 90° configuration. The evolution of NO was qualitatively revealed by its reaction with reduced myoglobin (Mb).^{7g,h} An argon stream was passed through the irradiated solution and collected afterwards in a *ca.* 1×10^{-6} M solution of Mb at pH = 7.2 (30 mM phosphate buffer), which was previously prepared by the reaction of metMb with sodium dithionite under argon. The coordination of NO to the Fe(II) center of Mb was monitored spectrophotometrically (Fig. S9†).^{7g,h} Numerical values for the quantum yields for the photoreactions (ϕ_{NO}) and deconvoluted spectral profiles of the

colored species were obtained by means of a chemometric procedure recently described elsewhere.¹⁷

The crystal structure of compound $[\text{1-NO}](\text{BF}_4)_2$ was determined using a Bruker-Nonius Kappa Mach3/APEX II diffractometer equipped with a Mo $\text{I}\mu\text{S}$ anode and INCOATEC Helios mirror optics ($\lambda = 0.71073$ Å). Diffraction data were collected at 100 K in a nitrogen cryo-stream. Final cell constants were obtained from least squares fits of several thousand strong reflections. Intensities of redundant reflections were used to correct for absorption using the SADABS program.¹⁸ The structure was readily solved by Patterson methods and subsequent difference Fourier techniques. The Siemens ShelXTL software package¹⁹ was used for solution and artwork of the structures, and ShelXL-2013²⁰ was used for structure refinement. All non-hydrogen atoms were anisotropically refined and hydrogen atoms bound to carbon were placed at calculated positions and refined as riding atoms with isotropic displacement parameters. The BF_4^- anions were found to be disordered on two positions. A split atom model with restrained atomic displacement parameters and bond lengths was refined using the ShelXL EADP, SADI and ISOR instructions. The occupation factor ratios refined to values of about 0.6 : 0.4 and 0.67 : 0.33, respectively. CCDC 1565106† contains the supplementary crystallographic data for this paper.

Theoretical calculations. All calculations reported in this paper were performed with the program package Gaussian 09.²¹ The geometry optimizations were carried out at the BP86 level²² of DFT. This functional has repeatedly proved to be reliable in predicting accurate structures of transition metal complexes. We employed the all-electron Gaussian basis sets reported by the Ahlrichs group. For all the atoms accurate triple- ζ valence basis sets with one set of polarization (TZV(P)) functions were used.²³ We employed tight SCF convergence criteria and default settings in the geometry optimizations. The nature of the resulting stationary points was in all cases tested by computing the vibrational spectra.

Results and discussion

Synthesis and characterization of $[\text{Fe}((\text{CH}_2\text{Py}_2)_2\text{Me}[9]\text{aneN}_3)(\text{NO})](\text{BF}_4)_2$ ($[\text{1-NO}](\text{BF}_4)_2$)

The pentadentate ligand $(\text{CH}_2\text{Py}_2)_2\text{Me}[9]\text{aneN}_3$ chosen for the preparation of the iron nitrosyl complex has already been employed in the preparation of acetonitrile complexes of Ru and Fe in the context of water oxidation catalyst investigation.²⁴ The strategy involved here in its preparation is different from the reported one, making its synthesis easier. Addition of the free ligand to a solution of $\text{Fe}(\text{BF}_4)_2 \cdot 5\text{H}_2\text{O}$ in $\text{CH}_3\text{CN}/\text{MeOH}$ under anaerobic conditions led to an immediate color change of the solution suggesting that the coordination had taken place at room temperature. Bubbling of $\text{NO}_{(\text{g})}$ into the ice cold mixture drastically turned the solution into almost black. Slow evaporation with an Ar stream yielded red prisms suitable for XRD investigation and allowed the isolation of the bulk product by treatment of the rest of the batch.

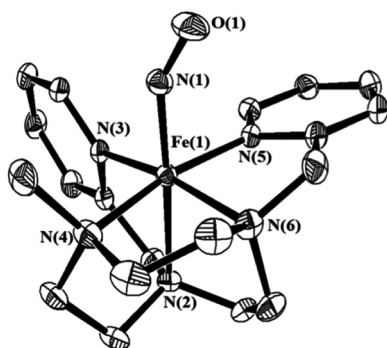


Fig. 1 Structure of the cation (30% probability level thermal ellipsoids) in the crystal of $[1\text{-NO}](\text{BF}_4)_2$.

The XRD investigation of the single crystals showed that the complex crystallizes in the chiral space group $P2_12_12_1$ with a unit cell comprised of four $[1\text{-NO}]^{2+}$ cations and eight BF_4^- anions (Fig. S5 and Table S1†). The counterions are partially disordered on two positions. The Fe^{2+} atom lies at the center of a distorted octahedron; the connectivity pattern and spatial distribution of the atoms in the first coordination sphere confirm the presence of the asymmetric geometric isomer (*asym* isomer) (Fig. 1), as was the case for other complexes reported with the same pentadentate ligand.²⁴ The refined Flack-parameter (0.017(5)) strongly supports that the correct absolute configurations have been determined and that the measured crystal was composed of just one enantiomer.²⁵

Table 1 reports the most significant structural parameters, together with those of the previously characterized $[1\text{-CH}_3\text{CN}](\text{OTf})_2$ species.^{24b} The substitution of CH_3CN by NO has strong implications. Whereas acetonitrile acts mainly as a σ -donor ligand, nitric oxide possesses the double effect of being both a σ -donor and π -donor, therefore strengthening the Fe–N(1) bond, which shortens from 1.929(2) Å in $[1\text{-CH}_3\text{CN}]^{2+}$ to 1.731(3) Å in $[1\text{-NO}]^{2+}$, while the *trans*-standing Fe–N(2) bond shows pronounced elongation from 1.992(2) Å in $[1\text{-CH}_3\text{CN}]^{2+}$

to 2.096(3) Å in $[1\text{-NO}]^{2+}$, which is caused by the NO-induced σ -*trans* effect. This behavior has been observed in other $\{\text{MNO}\}^7$ systems and is relevant in the field of bioinorganic chemistry.^{1,26} The $\{\text{FeNO}\}$ moiety is noticeably bent, with an Fe–N(1)–O(1) angle of 148.3(4)°, which is within the range characteristic of $\{\text{MNO}\}^7$ species (137°–155°).^{27,28} Particularly, bond lengths and angles agree well with those observed in $[\text{Fe}(\text{N}_3\text{PyS})(\text{NO})](\text{BF}_4)$ and $[\text{Fe}(\text{N}_4\text{Py})(\text{NO})](\text{BF}_4)_2$.¹⁰ The $\{\text{MNO}\}$ moiety also resembles the one in the only report of an hexacoordinated $\{\text{RuNO}\}^7$ species, $[\text{Ru}(\text{Me}_3[9]\text{aneN}_3)(\text{bpy})(\text{NO})](\text{BF}_4)_2$ ($[2\text{-NO}](\text{BF}_4)_2$).⁹ Table 1 also collects structural parameters for the DFT optimized structures of $[1\text{-NO}]^{2+}$ and $[1\text{-CH}_3\text{CN}]^{2+}$. Since $[\text{Fe}(\text{N}_3\text{PyS})(\text{NO})]^+$ revealed temperature-dependent high-spin ($S = 3/2$) and low-spin ($S = 1/2$) equilibrium,²⁹ the computations of $[1\text{-NO}]^{2+}$ have been performed considering both possibilities. The computed $S = 3/2$ spin state results 55 kJ mol^{−1} higher in energy than the $S = 1/2$ state. This fact combined with the comparison between the experimental and DFT optimized parameters tends to discard the high spin situation, which displays much longer Fe–N bond lengths than the experimental ones due to the presence of a HS Fe(II) center. Above all, DFT provides a deeper understanding of the electronic structure of the compound. The σ -*trans* effect arises from the partial delocalization of electronic density from the NO-centered π^* orbital into the metal centered d_{z^2} , and to a lower degree the d_{xz} orbital, all of which contribute to the SOMO of the molecule (Fig. 2, inset). The antibonding characteristic of this orbital with respect to the *trans* bond results in the elongation of the Fe–N(2) bond. In addition to these features, the IR spectrum of the species, collected by an ATR measurement shows an intense peak at 1660 cm^{−1} (Fig. S6†), computed by DFT at 1692 cm^{−1}, characteristic of the NO stretching vibration in $\{\text{MNO}\}^7$ octahedral species,^{27,28} and is in agreement with the significant π^*_{NO} nature of the SOMO, for it is a strong indicator of the presence of the unpaired electron in a mainly NO-centered orbital. This description is also compatible with the X-band EPR spectrum of $[1\text{-NO}]^{2+}$ recorded in a CH_3CN frozen glass at 30 K (Fig. 2), which confirms the spin state assignment. The spectrum shows the

Table 1 Selected experimental and calculated bond lengths, angles and NO stretching frequencies^a

	$[1\text{-NO}](\text{BF}_4)_2$ ^b	$[1\text{-NO}]^{2+}$ $S = 1/2$ ^c	$[1\text{-NO}]^{2+}$ $S = 3/2$ ^c	$[1\text{-CH}_3\text{CN}](\text{OTf})_2$ ^d	$[1\text{-CH}_3\text{CN}]^{2+}$ $S = 0$ ^c	$[1\text{-CH}_3\text{CN}]^{2+}$ $S = 2$ ^c
Distances/Å						
Fe–N(1)	1.731(3)	1.736	1.741	1.929(2)	1.891	2.117
Fe–N(2)	2.096(3)	2.145	2.226	1.992(2)	2.028	2.285
Fe–N(3)	1.987(3)	2.004	2.141	1.988(2)	1.972	2.153
Fe–N(4)	2.031(4)	2.108	2.265	1.994(2)	2.084	2.278
Fe–N(5)	1.992(3)	2.004	2.163	1.970(2)	1.994	2.183
Fe–N(6)	1.991(4)	2.027	2.246	2.047(2)	2.024	2.263
N(1)–O(1)	1.143(6)	1.183	1.170			
Angle/°						
Fe–N(1)–O(1)	148.3(4)	145.5	151.8	—		
$\nu_{\text{NO}}/\text{cm}^{-1}$						
	1660	1692	1765			

^a See Fig. 1 for atom labeling. ^b This work. ^c Computed employing DFT at the BP86/TZV(P) level of theory. ^d Ref. 24b.

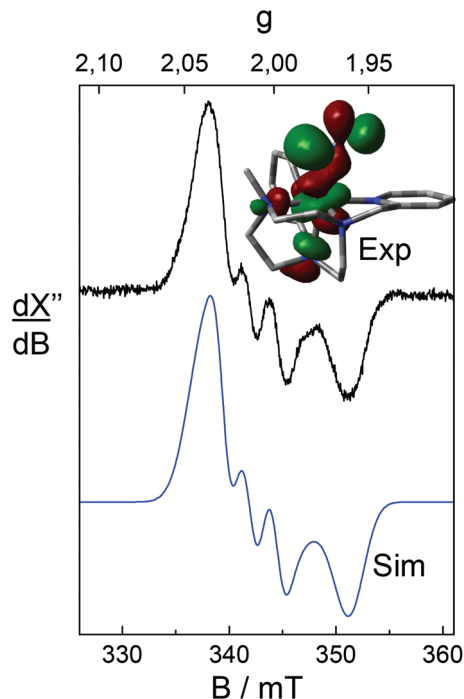


Fig. 2 X-band EPR spectrum of $[1\text{-NO}]^{2+}$ in 0.2 M $\text{CH}_3\text{CN}/[\text{Bu}_4\text{N}]\text{PF}_6$ at 30 K. Experimental conditions: Microwave frequency 9.6349 GHz, modulation of amplitude 1 G. Bottom: Computer-simulated spectrum (details in the text). Inset: Calculated SOMO of the species (DFT).

typical $S = 1/2$ signature of the $\{\text{MNO}\}^7$ fragment^{9,10,30,31} with rhombic g -values and hyperfine interaction with a single ^{14}N nucleus ($I = 1$). The simulation and fitting of the spectrum affords the spin-Hamiltonian g -values: $g = [2.0383 \pm 0.0003, 2.0137 \pm 0.0001, 1.9605 \pm 0.0001]$, and the diagonal values of the A -tensor: $A = [0.77 \pm 0.04, 23.89 \pm 0.06, 8.5 \pm 0.5] \times 10^{-4} \text{ cm}^{-1}$.

The electrochemical exploration by cyclic voltammetry in CH_3CN reveals two waves at 0.964 V and -0.327 V (vs. 3 M Ag/

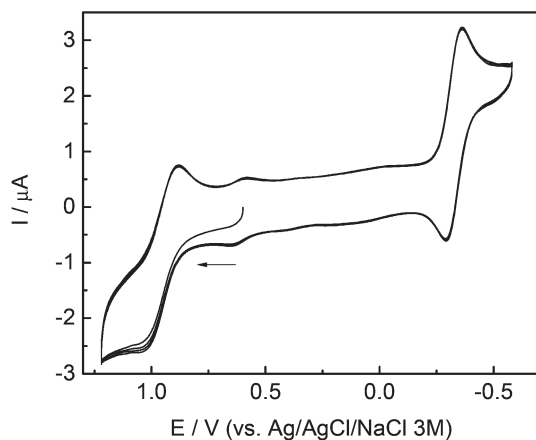


Fig. 3 Cyclic voltammogram of $[1\text{-NO}](\text{BF}_4)_2$ in $\text{CH}_3\text{CN}/0.2 \text{ M } [\text{Bu}_4\text{N}]\text{PF}_6$ at 298 K. Scan rate 100 mV s^{-1} . $E^{1/2}$ detected at 0.964 V and -0.327 V (vs. 3 M Ag/AgCl/NaCl).

AgCl/NaCl) (Fig. 3). Controlled potential coulometry and UV-vis spectroelectrochemistry confirm the one-electron nature of both processes. The spectral changes associated with the one-electron oxidation and reduction of $\{\text{FeNO}\}^7$ (Fig. 4 and Table S3†) are consistent with the previous reports of conversion into $\{\text{FeNO}\}^6$ and $\{\text{FeNO}\}^8$, respectively in related species.^{30,32}

Photochemical reactivity

When irradiated with a 450 nm light source, solutions of $[1\text{-NO}]^{2+}$ in acetonitrile undergo significant spectral changes, marked by the appearance of a new band in the visible range (400 nm) (Fig. 5) with the concomitant production of NO, which was detected qualitatively by its reaction with reduced myoglobin (Mb).^{7g,h} This pronounced variation of the absorption profile occurs with a well-defined isosbestic point, suggesting that the process can be interpreted as a clean conversion of the reagent into a single colored photoproduct. A multiwavelength chemometric analysis of the spectral changes¹⁷ in the region between 300 and 700 nm allowed us to calculate the concentration profile of the reaction and to deconvolute the spectrum of the product, which matches perfectly the one of $[1\text{-CH}_3\text{CN}]^{2+}$.^{24b} This suggests that $[1\text{-NO}]^{2+}$

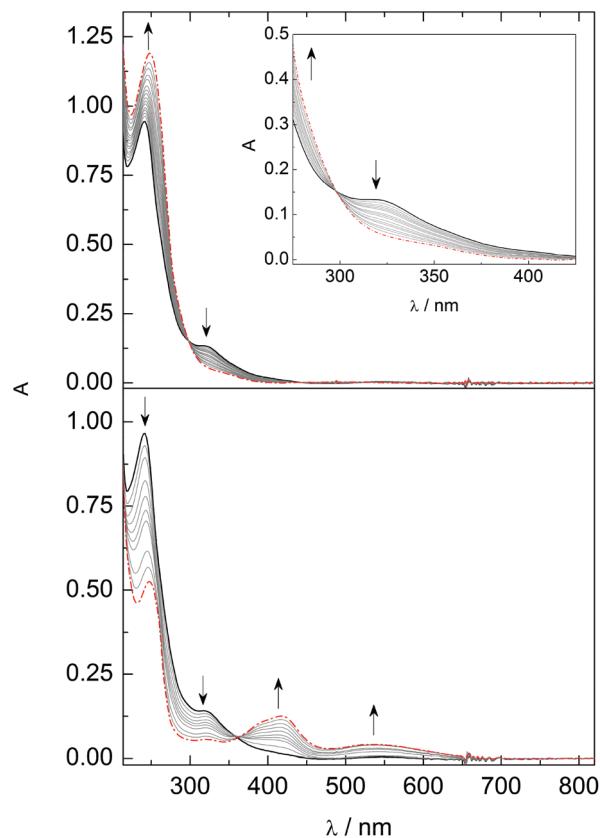


Fig. 4 UV-Vis spectra obtained by spectroelectrochemistry of $[1\text{-NO}](\text{BF}_4)_2$ in $\text{CH}_3\text{CN}/0.1 \text{ M } [\text{Bu}_4\text{N}]\text{PF}_6$ at 253 K under anaerobic conditions (Ar). Top: One-electron oxidation at 1.2 V vs. 3 M Ag/AgCl/NaCl (inset: zoom in). Bottom: One-electron reduction at -0.6 V vs. 3 M Ag/AgCl/NaCl.

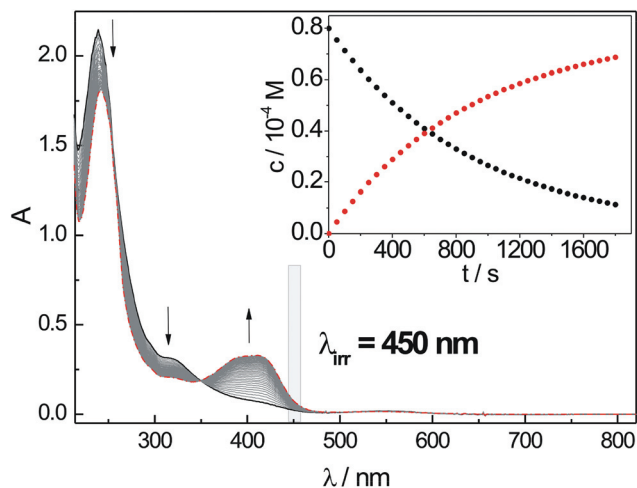


Fig. 5 Spectral changes in the UV-vis spectra of an acetonitrile solution of $[1\text{-NO}](\text{BF}_4)_2$ interacting with a light source ($\lambda_{\text{irr}} = 450 \text{ nm}$) under anaerobic conditions (Ar). Inset: Calculated concentration profiles for $[1\text{-NO}]^{2+}$ (black) and $[1\text{-CH}_3\text{CN}]^{2+}$ (red).

undergoes a rupture of the Fe–NO bond, photoreleasing a nitric oxide molecule, with the incorporation of a solvent molecule into the coordination sphere, as described in eqn (3):



This behavior parallels the one observed in the only photoactive $\{\text{FeNO}\}^7$ species reported in the literature.¹⁰ We don't detect any evidence of recombination of the photoreleased NO and estimate ϕ_{NO} as 0.52 mol einstein⁻¹, affording therefore a remarkably higher value than the values reported in the two photoactive $\{\text{RuNO}\}^7$ complexes reported previously: 0.15 mol einstein⁻¹ in the *cis*- $[\text{Ru}(\text{bpy})_2(4\text{-pic})]^{2+}$ from Sauaia *et al.* (in aqueous medium)⁸ and 0.09 mol einstein⁻¹ in $[2\text{-NO}]^{2+}$ in acetonitrile.⁹ When repeating the experiment with a 365 nm light source, the observed spectral changes are analogous and the estimated ϕ_{NO} becomes only slightly smaller (0.40 mol einstein⁻¹, Fig. S7†).

Conclusions

Whereas it is well established that $\{\text{MNO}\}^6$ species can easily photorelease NO by interaction with light of an appropriate wavelength, the photochemistry of $\{\text{MNO}\}^n$ ($n \neq 6$) species has so far been barely explored in the literature. This might lead to the wrong impression that these species are not accessible to the photorelease of NO. This above discussed new $\{\text{FeNO}\}^7$ species shows that the photodetachment of a nitric oxide molecule from an octahedral $\{\text{FeNO}\}^7$ compound is possible and most probably a normal process as for $\{\text{MNO}\}^6$ complexes. At this point, however, we cannot find a rational explanation to account for the lack of photoreactivity in $[\text{Fe}(\text{N}_4\text{Py})(\text{NO})]^{2+}$, though it is clear that the nature of the co-ligand environment may have a significant effect on the value of ϕ_{NO} . In any case,

this compound can be seen as a valuable example of a new kind of NO-photoreleasing system that deserves exploration, not only in connection to its bioinorganic relevancy, but also to provide insight into fundamental aspects of inorganic photochemistry. We seek to close this gap and a systematic study of related compounds with changes in the coordination sphere is underway to assess the effect these changes may have on the NO-photorelease quantum yield.

Conflicts of interest

There are no conflicts to declare.

Acknowledgements

This work has been supported by grants from CONICET, ANPCyT and the University of Buenos Aires (UBA). LDS is a member of the scientific staff of CONICET. NL and JP are doctoral fellows of the same institution. We wish to thank Dr A. Roitberg for providing access through collaboration to the computational resources of the National Center for Supercomputing Applications.

References

- 1 T. G. Traylor and V. S. Sharma, *Biochemistry*, 1992, **31**, 2847–2849.
- 2 E. Culotta and D. E. Koshland, *Science*, 1992, **258**, 1862–1865.
- 3 A. J. Hobbs, J. M. Fukuto and L. J. Ignarro, *Proc. Natl. Acad. Sci. U. S. A.*, 1994, **91**, 10992–10996.
- 4 (a) P. C. Ford, J. Bourassa, K. Miranda, B. Lee, I. Lorkovic, S. Boggs, S. Kudo and L. Laverman, *Coord. Chem. Rev.*, 1998, **171**, 185–202; (b) T. R. deBoer and P. K. Mascharak, *Adv. Inorg. Chem.*, 2015, **67**, 145–170.
- 5 M. J. Rose and P. K. Mascharak, *Coord. Chem. Rev.*, 2008, **252**, 2093–2114.
- 6 (a) E. Tfouni, M. Krieger, B. R. McGarvey and D. W. Franco, *Coord. Chem. Rev.*, 2003, **236**, 57–69; (b) M. G. Sauaia, F. D. Oliveira, A. C. Tedesco and R. S. da Silva, *Inorg. Chim. Acta*, 2003, **355**, 191–196; (c) A. G. De Candia, J. P. Marcolongo, R. Etchenique and L. D. Slep, *Inorg. Chem.*, 2010, **49**, 6925–6930.
- 7 (a) M. J. Rose, A. K. Patra, E. A. Alcid, M. M. Olmstead and P. K. Mascharak, *Inorg. Chem.*, 2007, **46**, 2328–2338; (b) M. J. Rose, M. M. Olmstead and P. K. Mascharak, *Polyhedron*, 2007, **26**, 4713–4718; (c) M. J. Rose and P. K. Mascharak, *Chem. Commun.*, 2008, 3933–3935; (d) G. M. Halpenny and P. K. Mascharak, *Inorg. Chem.*, 2009, **48**, 1490–1497; (e) C. G. Hoffman-Luca, A. A. Eroy-Reveles, J. Alvarenga and P. K. Mascharak, *Inorg. Chem.*, 2009, **48**, 9104–9111; (f) M. J. Rose and P. K. Mascharak, *Inorg. Chem.*, 2009, **48**, 6904–6917; (g) A. A. Eroy-Reveles, Y. Leung, C. M. Beavers, M. M. Olmstead and

- P. K. Mascharak, *J. Am. Chem. Soc.*, 2008, **130**, 4447–4458; (h) G. M. Halpenny, M. M. Olmstead and P. K. Mascharak, *Inorg. Chem.*, 2007, **46**, 6601–6606.
- 8 M. G. Sauer and R. S. da Silva, *Inorg. Chem. Commun.*, 2005, **8**, 347–349.
- 9 N. Levin, N. Osa Codesido, E. Bill, T. Weyhermuller, A. P. Segantin Faspari, R. S. da Silva, J. A. Olabe and L. D. Slep, *Inorg. Chem.*, 2016, **55**, 7808–7810.
- 10 A. C. McQuilken, Y. Ha, K. D. Sutherlin, M. A. Siegler, K. O. Hodgson, B. Hedman, E. I. Solomon, G. N. L. Jameson and D. P. Goldberg, *J. Am. Chem. Soc.*, 2013, **135**, 14024–14027.
- 11 W. L. F. Armarego and D. D. Perrin, *Purification of Laboratory Chemicals*, Reed Educational & Professional Publishing Ltd, 1996.
- 12 T. J. Atkins, *J. Am. Chem. Soc.*, 1980, **102**, 6364–6365.
- 13 G. R. Weisman, D. J. Vachon, V. B. Johnson and D. A. Gronbeck, *J. Chem. Soc., Chem. Commun.*, 1987, **20**, 886–887.
- 14 A. J. Dickie, D. C. R. Hockless, A. C. Willis, J. A. McKeon and W. G. Jackson, *Inorg. Chem.*, 2003, **42**, 3822–3834.
- 15 I. Noviantri, K. N. Brown, D. S. Fleming, P. T. Gulyas, P. A. Lay, A. F. Masters and L. Phillips, *J. Phys. Chem. B*, 1999, **103**, 6713–6722.
- 16 T. Lehoczki, É. Józsa and K. Ösz, *J. Photochem. Photobiol. A*, 2013, **251**, 63–68.
- 17 J. P. Marcolongo, J. Schmidt, N. Levin and L. D. Slep, *Phys. Chem. Chem. Phys.*, 2017, **19**, 21373–21381.
- 18 *SADABS-2014/5 - Bruker AXS area detector scaling and absorption correction*, Madison, WI, USA, 2014.
- 19 *ShelXTL, 6.14*, Madison, WI, USA, 2003.
- 20 G. M. Sheldrick, *ShelXL Version 2013/2*, Madison, WI, USA, 2013.
- 21 M. J. Frisch, *Gaussian 03, Rev. C.02 and D.01*, Wallingford CT, 2004.
- 22 (a) J. P. Perdew, *Phys. Rev. B: Condens. Matter*, 1986, **33**, 8822–8824; (b) A. D. Becke, *J. Chem. Phys.*, 1988, **84**, 4524–4529.
- 23 A. Schäfer, C. Huber and R. Ahlrichs, *J. Chem. Phys.*, 1994, **100**, 5829.
- 24 (a) C. Casadevall, Z. Codola, M. Costas and J. Lloret-Fillol, *Chem. – Eur. J.*, 2016, **22**, 10111–10126; (b) A. Company, G. Sabenya, M. González-Béjar, L. Gómez, M. Clémancey, G. Blondin, A. J. Jasiewicz, M. Puri, W. R. Browne, J.-M. Latour, L. Que, M. Costas, J. Pérez-Prieto and J. Lloret-Fillol, *J. Am. Chem. Soc.*, 2014, **136**, 4624–4633.
- 25 H. D. Flack, *Acta Crystallogr., Sect. A: Fundam. Crystallogr.*, 1983, **39**, 876–881.
- 26 (a) L. E. Goodrich and N. Lehnert, *J. Inorg. Biochem.*, 2013, **118**, 179–186; (b) A. P. Hunt and N. Lehnert, *Acc. Chem. Res.*, 2015, **48**, 2117–2125.
- 27 F. Roncaroli, M. Videla, L. D. Slep and J. A. Olabe, *Coord. Chem. Rev.*, 2007, **251**, 1903–1930.
- 28 (a) J. A. Olabe and L. D. Slep, in *Comprehensive Coordination Chemistry II, from Biology to Nanotechnology*, ed. J. A. Mc Cleverty and T. J. Meyer, Elsevier, Oxford, 2004, vol. 1, pp. 603–623; (b) S. E. Bari, J. A. Olabe and L. D. Slep, *Adv. Inorg. Chem.*, 2015, **67**, 87–144.
- 29 A. C. McQuilken, H. Matsumura, M. Dürr, A. M. Confer, J. P. Sheckelton, M. A. Siegler, T. M. McQueen, I. Ivanović-Burmazović, P. Moënné-Loccoz and D. P. Goldberg, *J. Am. Chem. Soc.*, 2016, **138**, 3107–3117.
- 30 (a) R. G. Serres, C. A. Grapperhaus, E. Bothe, E. Bill, T. Weyhermuller, F. Neese and K. Wieghardt, *J. Am. Chem. Soc.*, 2004, **126**, 5138–5153; (b) A. K. Patra, J. M. Rowland, D. Marlin, E. Bill, M. M. Olmstead and P. K. Mascharak, *Inorg. Chem.*, 2003, **42**, 6812–6823.
- 31 (a) S. Frantz, B. Sarkar, M. Sieger, W. Kaim, F. Roncaroli, J. A. Olabe and S. Zalis, *Eur. J. Inorg. Chem.*, 2004, 2902–2907; (b) M. Wanner, T. Scheiring, W. Kaim, L. D. Slep, L. M. Baraldo, J. A. Olabe, S. Zalis and E. J. Baerends, *Inorg. Chem.*, 2001, **40**, 5704–5707; (c) M. Videla, J. S. Jacinto, R. Baggio, M. T. Garland, P. Singh, W. Kaim, L. D. Slep and J. A. Olabe, *Inorg. Chem.*, 2006, **45**, 8608–8617.
- 32 C. Hauser, T. Glaser, E. Bill, T. Weyhermuller and K. Wieghardt, *J. Am. Chem. Soc.*, 2000, **122**, 4352–4365.